Structural properties of nanometre-sized ZnO crystals doped with Co

2007 J. Phys.: Condens. Matter 19 365223

(http://iopscience.iop.org/0953-8984/19/36/365223)

IOP PUBLISHING JOURNAL OF PHYSICS: CONDENSED MATTER

J. Phys.: Condens. Matter **19** (2007) 365223 (8pp) doi:10.1088/0953-8984/19/36/365223

Structural properties of nanometre-sized ZnO crystals doped with Co

N Hasuike[1], R Deguchi[1], H Katoh[1], K Kisoda[2], K Nishio[1], T Isshiki[1] and H Harima[1]

[1] Kyoto Institute of Technology, Matsugasaki, Sakyo-ku, Kyoto 606-8585, Japan
[2] Wakayama University, Wakayama 640-8510, Japan

E-mail: dj990074@djedu.kit.ac.jp (N Hasuike)

Received 2 December 2006, in final form 10 April 2007
Published 24 August 2007
Online at stacks.iop.org/JPhysCM/19/365223

Abstract

Nanometre-sized ZnO crystals doped with Co were synthesized by a co-precipitation method combined with a thermal treatment. By changing the reaction temperature, we can control the crystallite size from roughly 10 nm particles to 20 nm × 200 nm nm rods grown along the hexagonal *c*-direction. X-ray diffraction and Raman scattering showed growth of high-quality wurtzite ZnO crystals incorporating Co systematically in the ZnO host lattice in the tested range of [Co] < 3.0 mol%. Electronic transitions of Co in the oxygen tetrahedron were also observed in optical absorption, giving supporting evidence for systematic substitution of Co into the Zn site.

1. Introduction

Wide bandgap semiconductors lightly doped with magnetic elements (wide gap DMS; dilute magnetic semiconductors) have attracted much attention for realizing functional electronic devices based on the concept of spintronics. As a typical example, ZnO where a few per cent of Zn sites substituted by 3d-transition metals has been considered as one of the most promising candidates, since theoretical calculations have predicted room temperature ferromagnetism [1, 2]. Actually, many experiments have reported room temperature ferromagnetism in ZnO films doped with Co [3], V [4], Fe [5], Co with Fe [6] and so on. However, many papers have also appeared asserting that the ferromagnetism is a parasitic effect deriving from secondary phases such as segregated magnetic-element clusters [7]. Such controversial results probably appeared because the solubility of magnetic elements is very low, narrowing the process window for ideal alloy formation. Whatever the origin of the ferromagnetism, it is very true that the sample crystalline quality and the magnetic properties are sensitively dependent on the details of the processing conditions [8–11]. It is our strong belief that wide gap DMS should be critically characterized from the viewpoint of lattice

structure as well as magnetic properties, and, for that purpose, vibrational spectroscopy such as Raman scattering could be used as an ideal non-destructive characterization tool.

In this work we grew nanometre-sized ZnO crystals doped with Co and characterized them with emphasis on the sample quality (i.e. uniformity and, more importantly, substitution of Co to Zn sites), and sample reproducibility with controlled crystallite size and Co content. We have recently noticed that nanometre-sized wide gap DMS are attractive research objects for the following reasons: first, Sato *et al* [12], considering GaN-based DMS, found that low solubility of the magnetic element inevitably generated nanometre-sized islands of spinodal-decomposed phase, and a magnetic network of such islands rich in magnetic elements resulted in macroscopic ferromagnetic ordering at room temperature. Second, the relatively large surface to volume ratio in fine particles may release lattice-strain energies in doped materials, leading to an increase in solubility of the magnetic element [13]. Furthermore, quantum effects in nanometre-sized particles may also open up new fields.

There are also active discussions on ferromagnetic ordering in nanometre-sized ZnO-based DMS, concerning both positive [14–16] and negative [17–19] aspects: Cui *et al* [14] synthesized ZnO:Co nanowires with [Co] = 1–2% to observe magnetic hysteresis loops at room temperature and suggested the importance of structural rearrangement of Co for magnetic coupling by annealing at 400 °C (details unreported). Philipose *et al* [15] also grew ZnO:Mn nanowires with [Mn] = 1–4% to observe magnetic hysteresis, with $T_c > 400$ K. Jian *et al* [16] grew ZnO nanowires with post-growth ion-implantation of [Co] = 2–11% to observe magnetic hysteresis loops at 2 K in annealed samples. On the other hand, Luo *et al* [17] observed antiferromagnetic behavior in ZnO:Mn nanoparticles with [Mn] = 0.5–10%. Martinez *et al* [18, 19] also synthesized ZnO:Co nanoparticles with [Co] < 10%. They indicated by means of a detailed transmission electron microscopy (TEM) structural analysis that the intrinsic magnetic properties were closely connected to the sample microstructures: only uniform samples showed weak ferromagnetism at low temperature, while non-uniform and defective samples showed a paramagnetic character. They considered that in non-uniform samples a short Co–Co distance in Co-enriched regions promoted antiferromagnetic coupling and substantially reduced the overall magnetic moment. If vibrational spectroscopy were employed in these contrasting experiments, we could obtain a more clear-cut idea about the sample quality. Here, we would like to present such data for nanometre-sized ZnO crystals using high-resolution TEM observations.

2. Experiment

The sample was grown by a co-precipitation method by the reaction of Zn^{2+} and OH^- in alcoholic solution [20]. Doping of magnetic elements was carried out by the addition of Co^{2+} to the reaction. Two ethanolic solutions, one containing $Zn(NO_3)_2{\cdot}6H_2O$ and $Co(NO_3)_2{\cdot}6H_2O$, and the other containing NaOH, were slowly admixed and heated for 2 h in a closed vessel for crystal growth. The Co concentration and the heating temperature were varied in the range 0–3 mol% and 70–180 °C, respectively. The precipitates were separated from the solution, washed with distilled water repeatedly to remove $NaNO_3$ as a secondary product, and finally dried at 70 °C in an oven to obtain ZnO nanometre-sized crystals.

The surface morphology and crystallinity of the sample were observed by x-ray diffraction (XRD), TEM and selected area electron diffraction (SAED), and the sample composition was measured by energy dispersive x-ray (EDX) analysis. For vibrational spectroscopy, Raman scattering was observed at room temperature by a confocal microscope using a Ar^+ laser at 488.0 nm and a double monochromator equipped with a liquid N_2-cooled CCD (charge coupled

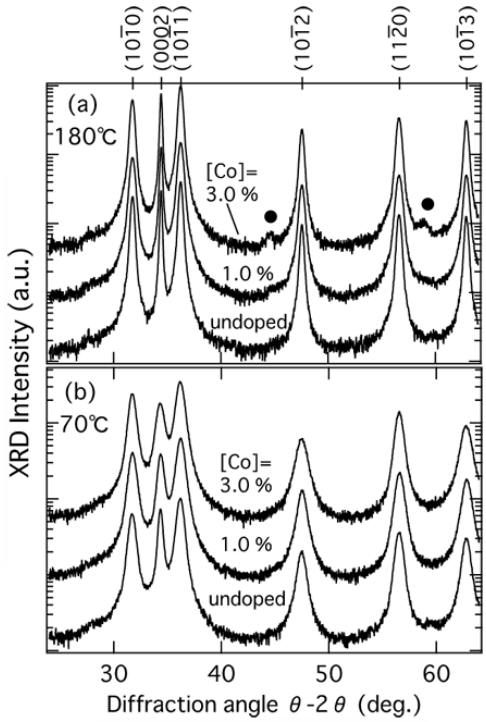

Figure 1. X-ray diffraction patterns of samples synthesized at 180 °C (a) and 70 °C (b). Co concentrations in mol% are denoted in the figure. Filled circles correspond to the secondary phase.

device) detector. Optical absorption measurement was also conducted at room temperature using a UV–visible–near-IR spectrophotometer.

3. Results and discussion

Figure 1 shows XRD patterns for samples grown at 180 °C (a) and 70 °C (b) with Co concentrations of [Co] = 0 (denoted as undoped), 1.0 and 3.0 mol%. All the XRD peaks were Miller-indexed using lattice constants of wurtzite ZnO, $a = 3.2495$ Å and $c = 5.2069$ Å [21], as shown in the figure. For the sample grown at 180 °C with [Co] = 3.0 mol%, however, a small contribution of impurity phase was observed at $2\theta = 44.69°$ and 58.69° as marked by filled circles. They probably originate from spinel-like phase Co_3O_4 or its isomorph $ZnCo_2O_4$ [22]. It is difficult to distinguish between them because they have the same crystal structure with very close lattice constants ($a \sim 8.0837$ Å). With the increase in growth temperature, the diffraction peaks become sharp, indicating growth in crystallite size and improvement in lattice ordering.

Figure 2 shows typical TEM images of samples grown at 70 °C with [Co] = 0 (a) and 3.0 mol% (b), and those grown at 180 °C with [Co] = 0 (c) and 3.0 mol% (d). The crystallite size and morphology are not affected by Co doping: The samples grown at 70 °C consist of uniform particles with dimension ∼10 nm, while those grown at 180 °C show a rod shape with width of ∼20 nm and length of 100–200 nm.

Figure 3 shows high-resolution TEM images (a, b) and EDX analysis (c) for a sample grown at 180 °C with [Co] = 3.0 mol%. Lattice fringes corresponding to alternating Zn and O stacking layers are clearly observed in (a) and its enlarged image (b). The inset in (a) shows its

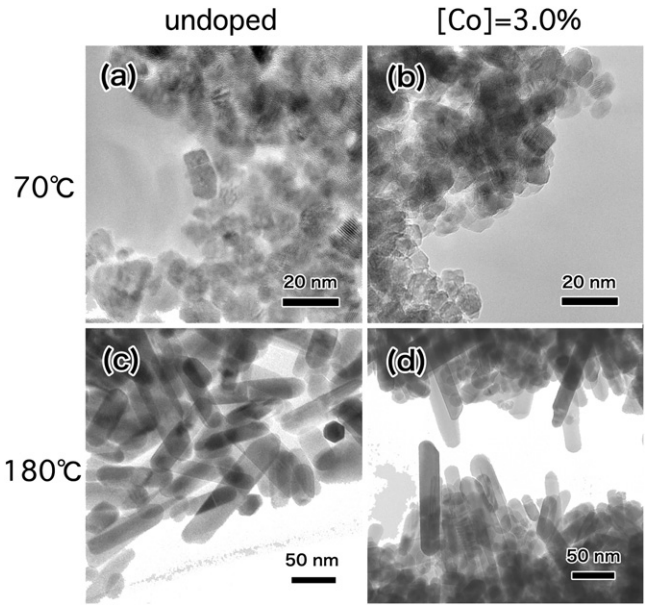

Figure 2. TEM image of samples grown at 70 °C ((a) undoped, (b) [Co] = 3.0 mol%) and 180 °C ((c) undoped, (d) [Co] = 3.0 mol%).

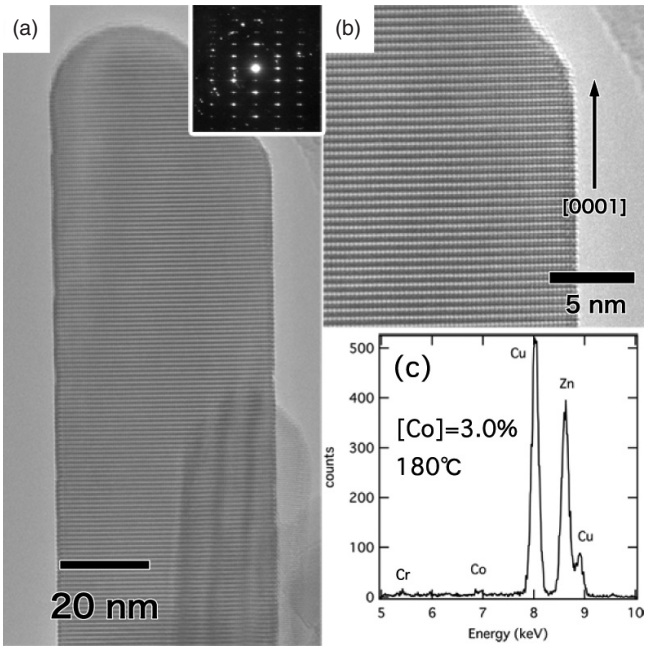

Figure 3. TEM image of a sample grown at 180 °C with [Co] = 3.0 mol% and its SAED pattern (a) and its magnified image (b). The EDX spectrum is shown in (c).

SAED pattern: it gives a typical electron diffraction pattern of wurtzite ZnO structure observed from the [11$\bar{2}$0] direction. These TEM and SAED patterns reveal that the rod sample is a

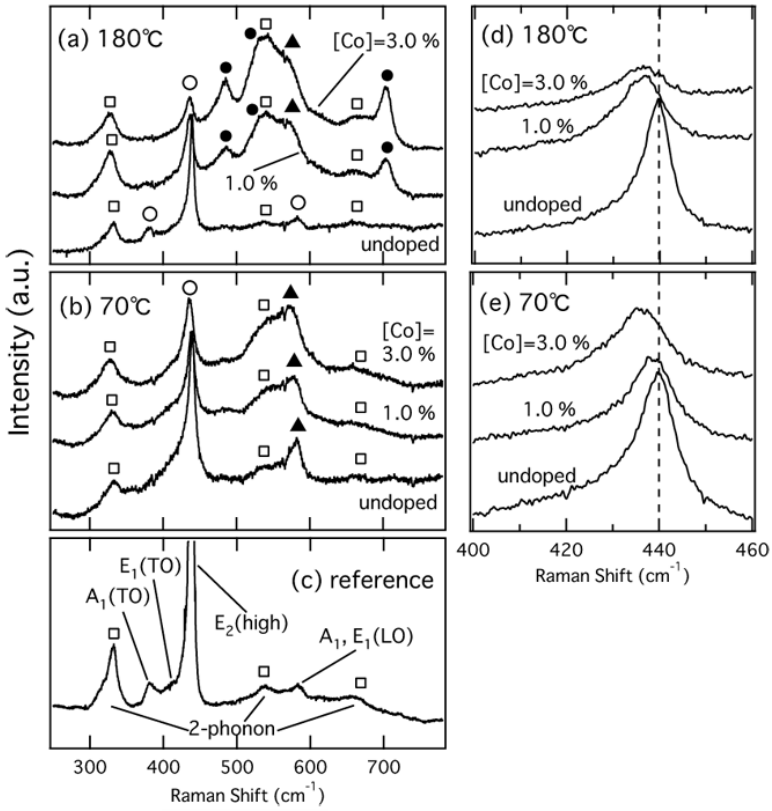

Figure 4. Raman spectra of samples grown at 180 °C (a) and 70 °C (b) with different Co contents. A reference spectrum of high-quality ZnO powder is shown in (c). The spectrum of the E_2 (high) phonon mode at ∼440 cm^{-1} is enlarged in (d) and (e) for 180 °C and 70 °C, respectively. Signals of the first-order phonon (open circle), second-order phonon (open square), defect (filled triangle) and secondary phase (filled circle) are recognized.

high-quality single crystal growing in the [0001] direction. The Co content in the rod sample was analysed by EDX as shown in (c), where the electron beam covered only the isolated rod crystal shown in (a). The Cr and Cu signals of (c) are an artefact coming from the sample holder. The Co peak at 6.94 keV was clearly discernible, and the intensity ratio to that of the Zn signal gives the Co content of a few mol% as expected from the sample recipe.

Figure 4 shows typical Raman spectra observed for samples grown at 180 °C (a) and 70 °C (b). The Co content is shown for each trace in the figure. For comparison, we observed a commercially available high-quality ZnO powder sample with sub-μm dimensions as shown in (c). Figures 4(d) and (e) are partial spectra enlarged from (a) and (b), respectively. ZnO has C_{6v} crystal symmetry and gives six Raman-active modes in the first-order phonon spectrum at 101, 380, 408, 438, 574 and 583 cm^{-1} for the E_2 (low), A_1 (TO), E_1 (TO), E_2 (high), A_1 (LO) and E_1 (LO) phonon modes, respectively [23]. The Raman spectra of ZnO have some unique features: the LO phonon signal is relatively weak [24] because two contributions, deformation potential and Frölich interaction of free carriers, act in the opposite direction in the Raman cross section. On the contrary, the two-phonon signal of ZnO (332, 541, and 660 cm^{-1}) is relatively strong [25] as seen in figure 4(c).

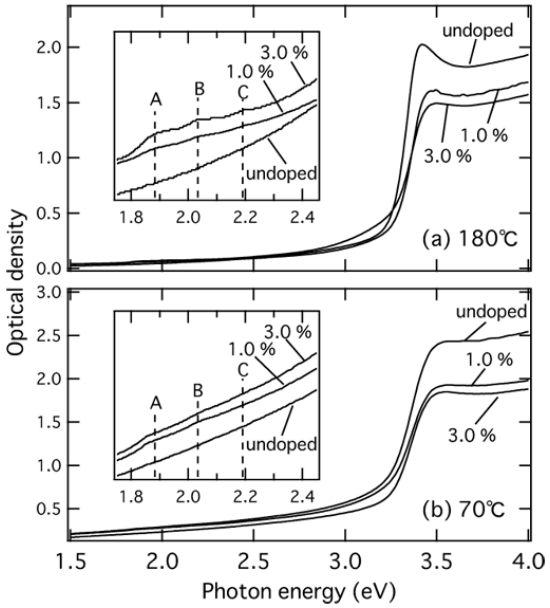

Figure 5. Optical absorption spectra for samples grown at 70 °C (a) and 180 °C (b). The inset shows vertical expansion at 1.8–2.4 eV.

The samples grown at 70 °C (figure 4(b)) give essentially the same spectra as (c), but as a small deviation a defect mode appears at 580 cm^{-1} even in the undoped sample and grows with increasing the Co concentration (filled triangle). This mode derives from defects such as O vacancies and is commonly observed in doped or ion-implanted films [26, 27]. As shown in figure 4(e), the most intense signal E_2 (high) at 440 cm^{-1} is very broad and tails to a lower frequency. With increasing Co content, this feature becomes more evident. The peak also shifts to a lower frequency. Since the crystallite size does not vary with the Co content, as seen in figure 2, the peak broadening is not explained by the 'nanometre-size effect' [28]. It is due to an 'alloying effect', [29], i.e. compositional fluctuation caused by random substitution of Co to Zn sites. The peak shift to a lower frequency with Co doping suggests lattice expansion.

The samples grown at 180 °C (figure 4(a)) show a similar variation to those grown at 70 °C (figure 4(b)). As a notable difference, however, additional peaks appear at about 485, 530 and 700 cm^{-1} for [Co] = 3.0 and 1.0 mol% (filled circles). Recalling that the XRD signal showed generation of a secondary phase in the sample grown at 180 °C with [Co] = 3.0 mol% (see figure 1(a)), the additional signals may derive from impurities like Co_3O_4 or $ZnCo_2O_4$. Better agreement of the impurity peak frequencies with those reported for Co_3O_4 [30] (483, 522, 691 cm^{-1}) than $ZnCo_2O_4$ [31] (∼470, 560, 690 cm^{-1}) suggests that Co_3O_4 is more probable in our case.

If the E_2 (high) mode at ∼440 cm^{-1} is closely compared for the samples grown at 180 °C (figure 4(d)) and 70 °C (figure 4(e)), the former gives a sharper peak as is evident in the undoped samples. Since there is no peak-frequency difference between the undoped samples for 180 °C and 70 °C, this difference is probably attributed to improved crystalline quality with the increase in growth temperature.

Figure 5 shows the optical absorption spectra at room temperature for the samples grown at 180 °C (a) and 70 °C (b). The 180 °C samples (a) are accompanied by exciton peaks at

∼3.4 eV. This is slightly larger than bulk ZnO (∼3.3 eV) [32], and can probably be attributed to a crystal size effect. Furthermore, three weak absorption peaks were observed at 1.88 (A), 2.02 (B) and 2.2 eV (C) in the Co-doped samples as seen in the vertically expanded traces (see insets). They correspond to electronic transition of Co 3d orbitals in the oxygen tetrahedron: $^4A_2(F) \rightarrow {}^2E(G)$, $^4A_2(F) \rightarrow {}^4T_1(P)$, and $^4A_2(F) \rightarrow {}^2A_1(G)$, respectively [33, 34]. These results again support the high crystalline quality of tested samples where Co ions occupy the Zn sites of host lattice.

4. Conclusion

Nanometre-sized ZnO crystals doped with Co were synthesized by a co-precipitation method with dimension of about 10 nm (particle) or 20 nm × 200 nm nm (rod) depending on the growth temperature. Characterization by XRD, TEM, Raman scattering and optical absorption showed that the synthesized crystals formed a high-quality wurtzite ZnO crystal lattice, incorporating Co ions systematically into the Zn site in the tested range of [Co] = 0–3.0 mol%. Sharp band-edge structures also evidenced the high crystalline quality of the samples.

Small impurity components such as Co_3O_4 appeared when synthesized at 180 °C with [Co] = 1–3 mol%. Our experiment showed, however, that such impurities can be suppressed by lowering the growth temperature to 70 °C. We believe that rigorous characterization of the sample crystallinity will clarify future discussions on the potential of ZnO for spintronics applications.

References

[1] Dietl T, Ohno H, Matsukura F, Cibért J and Ferrand D 2000 *Science* **287** 1019
[2] Sato K and Katayama-Yoshida H 2000 *Japan. J. Appl. Phys.* **39** L555
[3] Ueda K, Tabata H and Kawai T 2001 *Appl. Phys. Lett.* **79** 988
[4] Saeki H, Tabata H and Kawai T 2001 *Solid State Commun.* **120** 439
[5] Han S J, Song J W, Yang C H, Park S H, Park J H, Jeong Y H and Rhie K W 2002 *Appl. Phys. Lett.* **81** 4212
[6] Cho Y M, Choo W K, Kim H, Kim D and Ihm Y E 2002 *Appl. Phys. Lett.* **80** 3358
[7] Park J H, Kim M G, Jang H M, Ryu S and Kim Y M 2004 *Appl. Phys. Lett.* **84** 1338
[8] Janisch R, Gopal P and Spaldin N A 2005 *J. Phys.: Condens. Matter* **17** R657
[9] Özgür Ü, Alivov Y I, Liu C, Teke A, Reshchikiv M A, Dogän S, Avrutin V, Cho S-J and Morkoç H 2005 *J. Appl. Phys.* **98** 041301
[10] Pearton S J, Abernathy C R, Overberg M E, Thaler G T, Norton D P, Theodoropoulou N, Hebard A F, Park Y D, Ren F, Kim J and Boatner L A 2003 *J. Appl. Phys.* **93** 1
[11] Pearton S J, Heo W H, Ivill M, Norton D P and Steiner T 2004 *Semicond. Sci. Technol.* **19** R59
[12] Sato K, Katayama-Yoshida H and Dederichs P H 2005 *Japan. J. Appl. Phys.* **44** L948
[13] Samanta K, Bhattacharya P, Katiyar R S, Iwamoto W, Pagliuso P G and Rettori C 2006 *Phys. Rev.* B **73** 245213
[14] Cui J, Zeng Q and Gibson U J 2006 *J. Appl. Phys.* **99** 08M113
[15] Philipose U, Nair S V, Trudel S, de Souza C F, Aouba S, Hill R H and Ruda H E 2006 *Appl. Phys. Lett.* **88** 263101
[16] Jian W B, Wu Z Y, Huang R T, Chen F R, Kai J J, Wu C Y, Chiang S J, Lan M D and Lin J J 2006 *Phys. Rev.* B **73** 233308
[17] Luo J, Liang J K, Liu Q L, Liu F S, Zhang Y, Sun B J and Rao G H 2005 *J. Appl. Phys.* **97** 086106
[18] Martinez B, Sandiumenge F, Balcells Ll, Arbiol J, Sibieude F and Monty C 2005 *Phys. Rev.* B **72** 165202
[19] Martinez B, Sandiumenge F, Balcells Ll, Arbiol J, Sibieude F and Monty C 2005 *Appl. Phys. Lett.* **86** 103113
[20] Zhou H, Hofmann D M, Hofstaetter A and Meyer B K 2003 *J. Appl. Phys.* **94** 1965
[21] Heller R B, McGannon J and Weber A H 1950 *J. Appl. Phys.* **21** 1283
[22] Kolesnik S, Dabrowski B and Mais J 2004 *J. Appl. Phys.* **95** 2582
[23] Damen T C, Porto S P S and Tell B 1966 *Phys. Rev.* **142** 570
[24] Callender R H, Sussman S S, Selders M and Chang R K 1973 *Phys. Rev.* B **7** 3788
[25] Calleja J M and Cardona M 1977 *Phys. Rev.* B **16** 3753

[26] Hasuike N, Fukumura H, Harima H, Kisoda K, Matsui H, Saeki H and Tabata H 2004 *J. Phys.: Condens. Matter* **16** S5807
[27] Jouanne M, Morhange J F, Szuszkiewicz W, Golacki Z and Mycielski A 2006 *Phys. Status Solidi* c **3** 1205
[28] Campbell I H and Fauchet P M 1986 *Solid State Commun.* **58** 739
[29] Davydov V Yu, Goncharuk I N, Smirnov A N, Nikolaev A E, Lundin W V, Usikov A S, Klochikhin A A, Aderhold J, Graul J, Semchinova O and Harima H 2002 *Phys. Rev.* B **65** 125203
[30] Hadjiev V G, Iliev M N and Vergilov I V 1988 *J. Phys. C: Solid State Phys.* **21** L199
[31] Samanta K, Bhattacharya P and Katiyar R S 2007 *Phys. Rev.* B **75** 035208
[32] Teke A, Özgür Ü, Doğan S, Gu X, Morkoç H, Nemeth B, Nause J and Everitt H O 2004 *Phys. Rev.* B **70** 195207
[33] Jin Z, Fukumura T, Kawasaki M, Ando K, Saito H, Sekiguchi T, Yoo Y Z, Murakami M, Matsumoto Y, Hasegawa T and Koinuma H 2001 *Appl. Phys. Lett.* **78** 3824
[34] Koidl P 1977 *Phys. Rev.* B **15** 2493